ELSEVIER

Nuclear Instruments and Methods in Physics Research B 157 (1999) 183–190

NIM B
Beam Interactions with Materials & Atoms

www.elsevier.nl/locate/nimb

Quantum-resolved electron stimulated interface reactions: D_2 formation from D_2O films

T.M. Orlando *, G.A. Kimmel, W.C. Simpson [1]

W.R. Wiley, Environmental Molecular Sciences Laboratory, Pacific Northwest Nat. Laboratory, Richland, WA 99352, USA

Abstract

The low-energy (5–15 eV) electron stimulated desorption of D^- and D_2 ($^1\Sigma_g^+$, $v=0$, $J=0$ and $v=1$, $J=2$) from condensed D_2O films is investigated as a function of substrate temperature. The D^- ions are produced primarily via the $^2B_1$ dissociative electron attachment resonance. Both the D^- and D_2 yields are enhanced when the substrate temperature increases from 90 to 140 K. The changes in the D^- and D_2 yields with substrate temperature are qualitatively similar. We attribute the increase in yields to thermally induced rotations or breaks in the near-surface hydrogen bonding network. This reduction in co-ordination and coupling reduces the nearest neighbor perturbations and enhances the surface or near surface excited state lifetimes. Production of vibrationally excited D_2 molecules correlates with reactive scattering of D^- at the surface, whereas production of D_2 in the $v=0$ level also includes molecular elimination from an excited state which is produced by autodetachment.

PACS: 79.20.Kz; 33.80.Rv; 34.80.Gs
Keywords: Ion–surface interactions; Electron stimulated desorption (ESD); Water; Desorption induced by electronic transitions (DIET)

1. Introduction

It is well known that the impact of high energy ions and electrons with materials and interfaces produces low-energy (<100 eV) secondary electrons [1–4]. It has also been experimentally established that the maximum secondary electron emission yield for uncharged insulator surfaces, δ_m^o, is generally much greater than 1.0 and, in the case of wide band-gap insulating materials, δ_m^o can exceed 20. The energy distributions of the emitted electrons generally peak at a few eV, however, the distributions are typically very broad so a considerable number have energies which extend out to >50 eV. When adsorbate layers or liquids are present at ion or electron bombarded surfaces and interfaces, the emitted secondary electrons from the solid targets must undergo multiple inelastic

* Corresponding author. Tel.: +1-509-376-9420; fax: +1-509-376-6066; e-mail: thomas.orlando@pnl.gov
[1] Associated Western Universities Postdoctoral Fellow.

0168-583X/99/$ – see front matter
PII: S0168-583X(99)00436-X

scattering events as they traverse the interfacial molecular layers prior to trapping or solvation.

The primary energy-loss channels for electrons with energies typical of the secondary distribution are ionization (electron-hole pair production in the condensed phase), direct electronic excitation and resonance scattering. The latter results in the formation of transient negative ion resonances which decay via electron autodetachment and dissociative electron attachment (DEA). DEA usually involves multielectron core-excited resonances which consist of an excess electron temporarily bound by the positive electron affinity of an electronically excited target molecule. These are generally two-electron, one-hole configurations that are classified as either Feshbach or core-excited shape resonances. Since the lifetimes of Feshbach resonances are typically $\sim 10^{-12}$–10^{-14} s, dissociation into stable anion and neutral fragments may result if the resonance is dissociative in the Franck–Condon region and one fragment has a positive electron affinity. DEA has been observed in the condensed-phase, and many body interactions affect the resonance energies, widths and lifetimes [5–13]. Important aspects of condensed-phase DEA which have received relatively little attention are substrate temperature effects [11–13] and the subsequent post-dissociation interactions of the anion fragments with the surrounding medium [14,15].

In this paper, we investigate the inelastic scattering of electrons whose energy distribution is typical of secondary electrons produced by high energy ion or electron impact. We extend earlier work on the temperature dependencies of DEA in nanoscale ice films [11–13] and demonstrate that the yields of D^- and D_2 produced between 5–15 eV incident energies increase with substrate temperature. We propose that the increased ion yield results from hydrogen bond breaking near the surface, which reduces the perturbation of the $4a_1$ antibonding level of the surface water molecules, thereby enhancing the lifetimes of the dissociative excited states that lead to ion desorption. The production of vibrationally excited D_2 molecules seems to correlate with reactive scattering of D^- at the surface, whereas production of D_2 in the $v=0$ level also involves a molecular elimination step [10].

2. Experimental procedure

The experiments were carried out in an ultra-high vacuum (UHV) chamber (base pressure $\sim 2\times 10^{-10}$ Torr) equipped with a pulsed low-energy electron gun, an effusive gas doser, a quadrupole mass spectrometer (QMS), a time-of-flight (TOF) detector and a Pt(111) crystal mounted on a liquid-nitrogen-cooled manipulator. The Pt crystal was cleaned by repeatedly heating it in O_2 (5×10^{-8} Torr) and then in UHV. Film temperature was measured using a K-type thermocouple, and has an estimated accuracy of ±5 K.

Ice films were grown via vapor deposition of D_2O and thickness was determined by comparing D_2O temperature programmed desorption (TPD) spectra to published data [16–18], and has an estimated accuracy of ~20%. Coverages are reported in terms of ice bilayers ($\sim 10^{15}$ molecules/cm^2). D^- ions were generated by a monoenergetic electron beam, with an energy spread of ~0.3 eV full-width at half-maximum (FWHM), and collected in the TOF spectrometer. The incident electron beam was pulsed at 100 Hz, with a pulse length of 1 μs and an instantaneous current of $\sim 10^{-7}$ A in a spot size of ~0.1 cm^2, resulting in a time-averaged current density of $\sim 10^{-10}$ A/cm^2. The very low incident electron flux used in these experiments results in negligible charging or thermal heating of the substrate [10–18]. For the temperature dependence measurements, the ice films were heated radiantly using a tungsten filament mounted behind the Pt crystal.

We have utilized (2 + 1) resonance enhanced multiphoton ionization (REMPI) via the E, F $^1\Sigma_g^+$ state to detect the D_2 products in the (X $^1\Sigma_g^+$) ground state [19]. The laser wavelengths necessary for this detection scheme were generated by frequency tripling the output of a Nd:YAG pumped dye laser. Typical output power ranged from 1–2 mJ/pulse and our estimated detection efficiency is $\sim 10^6$ molecules/cm^3/quantum state. All laser experiments were done in the TOF mode in which the neutrals produced by the pulsed electron-beam traverse a 4 mm distance before they are resonantly ionized by the focused laser beam. Due to the small signal levels in these experiments, it was not possible to measure the velocity distribution of

the D_2 molecules desorbing from the ice. Instead, a relatively long (~20–25 μs) electron beam pulse (20 Hz) was used which integrates a range of desorbate velocities. The ionizing laser pulse was delayed with respect to the electron beam pulse such that the D_2 molecules detected had translational energies <0.5 eV.

3. Results and discussion

3.1. Condensed-phase DEA resonances

The energy dependence of the D^- ESD yield from a 5-bilayer thick amorphous solid water film of D_2O on Pt(111) at 120 K is illustrated in Fig. 1. (The film thickness and temperature were chosen to maximize the resolution of the D^- signal.) The D^- yield rises significantly in the interval between 5–14 eV and the TOF baseline, which contains contributions from scattered electrons and D^- production via dipolar dissociation, gradually increases. The signal peaks at ~7 eV, with a shoulder at ~9 eV and a slightly less intense feature at ~11 eV. As shown in Fig. 1, a sum of three Gaussian peaks and a linearly increasing background fits this data reasonably well.

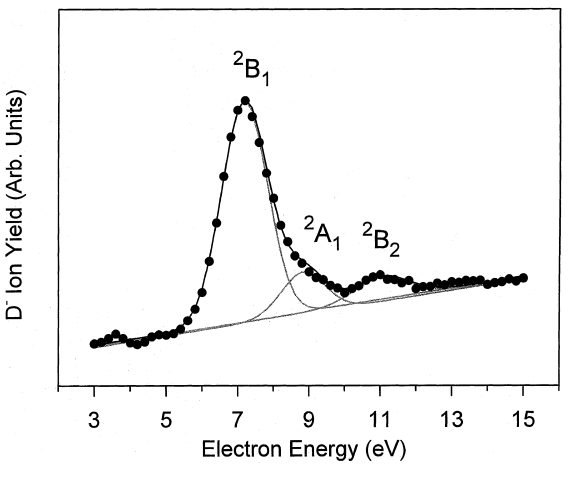

Fig. 1. D^- signal vs. incident electron energy, collected at 120 K from a five-bilayer film of amorphous ice, which was grown at 90 K. The solid lines are Gaussian fits to the data.

The ground state electronic structure of an isolated water molecule is $(1a_1)^2(2a_1)^2(1b_2)^2(3a_1)^2(1b_1)^2$, where the $1a_1$ orbital is essentially the O(1s) core level, the $2a_1$ and $1b_2$ orbitals are primarily involved in O–H bonding, and the $3a_1$ and $1b_1$ are non-bonding lone-pair orbitals [20]. The lowest-lying unoccupied orbital is the $4a_1$ [20]. This strongly antibonding orbital mixes with the 3s Rydberg state [21], and hence is denoted as $(3s{:}4a_1)$. The $^2B_1$, $^2A_1$ and $^2B_2$ DEA resonances, which correspond to states having two $(3s{:}4a_1)$ electrons and a hole in the $1b_1$, $3a_1$ or $1b_2$ orbital, respectively, have been observed in water vapor [22–24]. The antibonding nature of the $(3s{:}4a_1)$ orbital makes these excited states highly dissociative. Much of the 3s Rydberg character of this level appears to be lost upon condensation due to short-range interactions between neighboring molecules. However, this level retains its dissociative nature in the condensed phase due to the antibonding $4a_1$ configuration and thus the first two peaks in Fig. 1 are assigned as the $^2B_1$ and $^2A_1$ resonances. These resonances are known to generate measurable ion yields in the ESD of condensed water films [8–13]. The third feature, at ~11 eV, is only resolvable at very low current densities and is assigned as the $^2B_2$ resonance [11,12]. At higher current densities, the $^2B_1$ and $^2A_1$ resonance widths increase [12,13], obscuring the structure near 11 eV.

3.2. Temperature dependence of D^- desorption

Since DEA involves localized scattering events, excited-state lifetimes (and hence DEA cross sections) are expected to be sensitive to the local potential which, in turn, will vary with the film's morphology and temperature. This should be evident in condensed water films, where short-range interactions between neighboring molecules perturb the electronic structure [8–13,25,26]. To investigate this, we measured the temperature dependence of the negative-ion ESD yield from amorphous solid water films. Fig. 2 shows the D^- yield from a 60 bilayer thick film of amorphous D_2O at several temperatures. (Note the data in Fig. 2 have been offset vertically for display with the zero signal levels defined as the intensity at the lowest incident electron energy.) At low

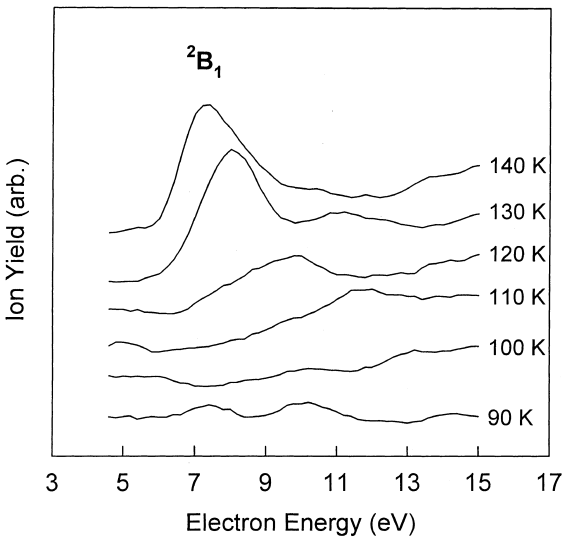

Fig. 2. Temperature dependence of the D^- signal vs. incident electron energy from a sixty-bilayer film of amorphous ice. The film was initially grown at 90 K and the data was collected with the film held at the various temperatures indicated. The data is offset vertically for display.

temperatures, the D^- yield from these relatively thick films is very small and the contributions from the $^2B_1$, $^2A_1$ and $^2B_2$ DEA resonances seem comparable. This is in contrast to the thin-film (~5-bilayer) data presented in Fig. 1. The lower D^- signal at coverages greater than ~5-bilayers may indicate that the surface of a thick film is structurally different from that of a thin film. Water initially adsorbs on a clean Pt surface with its oxygen preferentially oriented toward the metal, forming a structure ordered in at least one dimension, and possibly in two or three [27]. For thicker ice films at lower temperatures, molecular dynamics simulations predict that most of the surface molecules have their hydrogen bonds parallel to or pointing into the surface [27].

In the case of thicker films, the D^- yield begins to increase as the temperature is raised and the position of the resonances shift to lower incident electron energies (see Fig. 2). These effects are greatest for the $^2B_1$ resonance and occur at temperatures where thermal desorption is negligible and prior to the amorphous to cubic phase transition in the film [17]. One explanation for the increase in the D^- yield with temperature is that the number of dangling hydrogen bonds increases as the temperature increases. This change in the average orientation of water molecules on the surface is supported by measurements which show that the work function of amorphous solid water [relative to the Pt(111) substrate] decreases as the temperature increases [28].

A similar temperature dependence was observed in the ESD yield of low-kinetic-energy D^+ from D_2O ice [26]. The rise in D^+ ESD yield with temperature was attributed to thermally activated reduction in surface hydrogen bonding. One possible mechanism for thermally induced hydrogen bond breaking near the surface is the mobilization of *pre-existing* L- or D-defects (i.e., disrupted hydrogen bonds). The energy required to directly break a hydrogen bond (~0.25 eV) is too high for significant bond breaking to occur spontaneously at the temperatures where the ESD yield begins to rise. However, in a typical ice film, there are a large number of pre-existing defects that form as the film is grown. The volume density of these defects can be as high as $\sim 10^{19}$ cm^{-3} near the surface [29], yielding an area density of 10^{12}–10^{13} cm^{-2} (roughly one defect for every 10^2–10^3 surface molecules). Using infra-red absorption spectroscopy techniques, Devlin et al. observed that the onset for defect mobility occurs at around 100 K for amorphous ice [30], which is consistent with the increased ESD yield (Fig. 2) we observe at higher temperatures. Changes in the ESD yield with temperature may also be associated with processes such as sintering (i.e. an increase in the density of the ice) [25,31]. Though the mechanism of sintering is not well understood, self-diffusion, surface diffusion and/or mobilization of defects to the surface would temporarily break hydrogen bonds [25,31].

As the temperature increases, the threshold for the formation of D^- shifts to lower energies (Fig. 2) which are closer to the values observed for gas-phase DEA [22–24]. As discussed below, the shift to lower energies is also consistent with changes in the orientation of the surface water molecules. DEA resonances in the condensed phase can be shifted to higher energies due to repulsive interactions with neighboring molecules. For example,

in the case of the $^{3,1}B_1$ ($1b_1 \rightarrow 4a_1$) Frenkel exciton, (i.e. the parent state of the $^2B_1$ DEA resonance), there is a repulsive interaction between the oxygen atom of the excited water molecule and the surrounding waters due to the fact that the dipole moment of the water excited state is opposite in direction to the dipole moment of the ground state [32,33]. Thus, the positive charge density near the excited oxygen repels the positive charges of ground state hydrogen atoms involved in hydrogen bonding. There is also an enhanced exchange repulsion which comes from the large spatial extent of the Frenkel-type exciton wavefunction. In view of these repulsive interactions, it is expected that DEA resonances for highly coordinated or sub-surface sites will be shifted to higher energies relative to those at the surface. Conversely, it is also expected that a reduction in the hydrogen bonding interactions will cause a shift to lower energy due to a reduction of the perturbations.

Disruption of the near surface hydrogen bonding would increase the lifetimes and localization probabilities of the excited states responsible for ion desorption, especially those excited states that involve the levels of ice which participate in hydrogen bonding [26]. In fact, Rosenberg et al. has shown that excitations involving the lowest-lying $4a_1$ orbital *only* survive at the surface due to the reduced coordination of the surface molecules, and that these excitations lead to enhanced ion desorption [34]. Since the excitation that lead to D^- and low-energy D^+ desorption involve occupation of the $4a_1$ level [26], it is likely that thermally induced changes in the lifetimes of excited states involving this level are partially responsible for the changes in ESD yields with temperature.

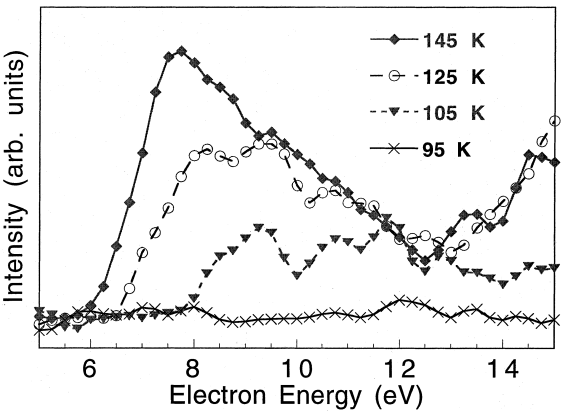

Fig. 3. Temperature dependence of the D_2 ($v=1$, $J=2$) signal vs. incident electron energy from a sixty-bilayer film of amorphous ice. The films were initially grown at 90 K and the data was collected with the films held at the various temperatures indicated.

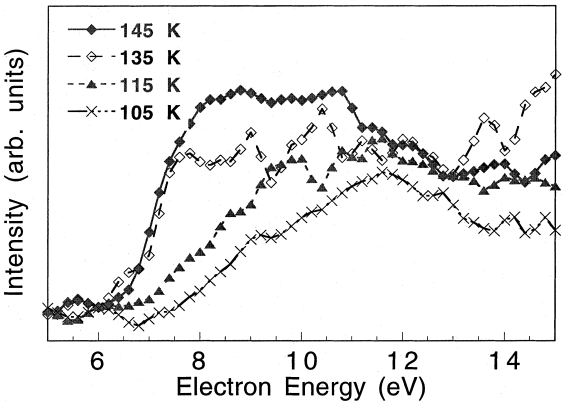

Fig. 4. Temperature dependence of the D_2 ($v=0$, $J=0$) signal vs. incident electron energy from a sixty-bilayer film of amorphous ice. The films were initially grown at 90 K and the data was collected with the films held at the various temperatures indicated.

3.3. D_2 production and D^- reactive scattering

The temperature dependence of the electron-stimulated production and desorption of D_2 in the $v=1$, $J=2$ and $v=0$, $J=0$ levels are shown in Figs. 3 and 4, respectively. At low temperatures (i.e. 90–95 K), there is no D_2 signal above our detection sensitivity ($\sim 10^6$ molecules/cm^3/quantum state) in the $v=1$, $J=2$ levels [10]. However, the yield of the D_2 in the $v=1$, $J=2$ levels clearly increases when the substrate is heated above 100 K and the peak shifts to low incident electron energies in a manner which is similar to the changes observed in the D^- yield as a function of temperature. A similar, though less pronounced increase and shift in resonance energy, is observed for the D_2 in the $v=0$, $J=0$ levels. The shift is less pronounced since the low temperature signal which is peaked at $\sim$11 eV, persists but is temperature

independent. The D_2 ($v=0$, $J=0$) yield in this energy range has been associated with direct molecular elimination from the $^2B_2$ DEA resonance or excited states produced by autodetachment [10].

The data in Figs. 3 and 4 suggest that the production of D_2 at temperatures above 100 K may involve reactive scattering of the D^- species which is produced via DEA. To show this more clearly, we directly compare the D^- yield at 140 K with the yield of D_2 in the $v=1$, $J=2$ and $v=0$, $J=0$ levels at elevated temperatures in Figs. 5 and 6, respectively. The data are normalized to the peak maxima to allow comparison. It is clear that the general shape of the yield of vibrationally excited D_2 as a function of incident electron energy compares favorably with the yield of D^-. There is a very slight shift in the threshold energy and a broadening for incident electron energies above ~8 eV. The comparison for the yield of D_2 in the vibrationally and rotationally relaxed levels ($v=0$, $J=0$) is similar but the correlation with the D^- desorption yield is not as good. For example, the maximum D_2 signal clearly peaks at a higher energy and is much broader than the D^- desorption maxima. The threshold is also shifted by at least 0.75 eV. These important differences are reproducible and are not due to charging since the fluxes

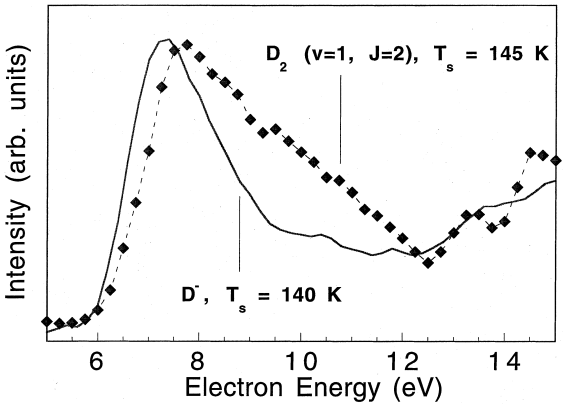

Fig. 5. Comparison of the D^- yield vs. incident electron energy with the D_2 ($v=1$, $J=2$) signal. Data was obtained from a sixty-bilayer film of amorphous ice grown at 90 K and then heated to ~140 ± 5 K.

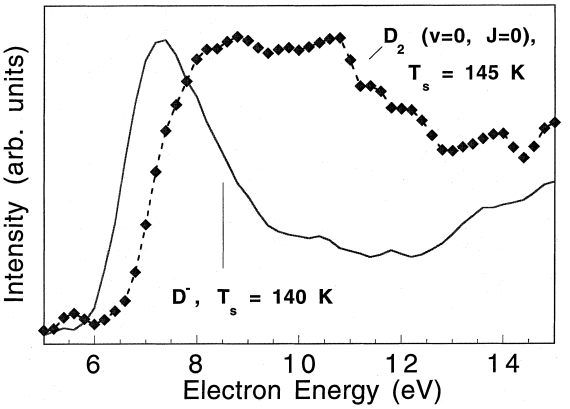

Fig. 6. Comparison of the D^- yield vs. incident electron energy with the D_2 ($v=0$, $J=0$) signal. Data was obtained from a sixty-bilayer film of amorphous ice grown at 90 K and then heated to ~140 ± 5 K.

used were at least an order of magnitude below the conditions known to produce charge build-up [13]. In addition, investigations of the yield of atomic D and O under similar conditions produced no comparable shifts in the yields vs energy as the sample temperature was changed [35]. We suggest that the broad signal is due to a convolution of the direct, temperature independent channel centered at 11 eV, and a contribution from D^- reactive scattering which grows in with temperature. The higher threshold energy may be indicative of D^- reactive scattering in sub-surface layers followed by multiple scattering prior to desorption. This is consistent with the near complete lack of vibrational and rotational energy.

The exothermic (ΔH_g = gas-phase reaction enthalpy) proton transfer reaction

$$D^- + D_2O \rightarrow D_2 + OD^- \quad \Delta H_g = -0.45 \text{ eV} \qquad (1)$$

has been studied in the gas-phase and is assumed to proceed via the formation of a proton-bound intermediate complex [36] which may resemble D-defects in ice. Evidence for this reaction has also been presented in studies of low-energy electron attachment to van der Waals clusters of D_2O (H_2O) [37,38]. The cluster ion distributions observed using 6–12 eV electrons were interpreted in terms of DEA initiated intra-cluster ion-molecule half reactions such as $(H^-)\ (H_2O)_{n-1} \rightarrow (OH^-)$

$(H_2O)_{n-2} + H_2$ [37,38]. This reaction may be enhanced in the condensed phase due to the large number of collision partners and the increased exothermicity resulting from ion solvation.

It is very likely that the vibrationally excited D_2 molecules shown in Figs. 3 and 5 and most of the D_2 ($v=0$, $J=0$) between 6 and 9 eV are produced primarily via reactive scattering of D^- on the surface of the amorphous solid water film. In this case, the D^- is produced mainly via the $^2B_1$ resonance. However, the broad D_2 ($v=1$, $J=2$) yield which 'turns on' between 8–12 eV at 105 K and persists at 145 K, may involve reactive scattering of D^- which is produced by either the $^2A_1$ or $^2B_2$ resonances or both.

4. Summary

We have investigated the low-energy (5–15 eV) electron stimulated desorption of D^- and D_2 ($^1\Sigma_g^+$, $v=0$, $J=0$ and $v=1$, $J=2$) from condensed D_2O films as a function of substrate temperature. The D^- ions are primarily produced via the $^2B_1$ dissociative electron attachment resonance. Both the D^- and D_2 yields increase when the substrate temperature increases from 90 to 140 K. We attribute the increase in the ion yield to thermally induced rotations or breaks in the near-surface hydrogen bonding network. This reduction in the co-ordination and coupling strength enhances the lifetimes (or reduces the decay rates) of the excited states that lead to D^- production. Production of vibrationally excited D_2 molecules seems to correlate with reactive scattering of D^- at the surface, whereas production of D_2 in the $v=0$ level likely involves a molecular elimination step and some subsurface D^- reactive scattering. A more detailed study of the D^- reactive scattering process is underway since it represents the opportunity to perform a state-to-state mapping study of an ion–molecule reaction at an interface.

Acknowledgements

The work was supported by the U.S. Department of Energy (DOE), Office of Basic Energy Sciences, Chemical Physics Program. It was performed at the W. R. Wiley Environmental Molecular Sciences Laboratory, a national scientific user facility sponsored by the U.S. DOE Office of Biological and Environmental Research and located at Pacific Northwest National Laboratory (PNNL). PNNL is operated for the DOE by Battelle under contract No. DE-AC06-76RLO 1830.

References

[1] K. Kanaya, S. Ono, F. Ishigaki, J. Phys. D: Appl. Phys. 11 (1978) 2425 and references therein.
[2] H. Seiler, J. App. Phys. 54 (1983) R1 and references therein.
[3] J.P. Ganachaud, A. Mokrani, Surf. Sci. 334 (1995) 329.
[4] J. Cazaux, J. App. Phys. 85 (1998) 1137.
[5] L. Sanche, in: C. Ferrandi, J.P. Jay-Gerin (Eds.), Excess Electrons in Dielectric Media, CRC Press, Boca Raton, 1991, ch. 1.
[6] L. Sanche, A.D. Bass, P. Ayotte, I.I. Fabrikant, Phys. Rev. Lett. 75 (1995) 3568.
[7] L. Sanche, Scanning Microscopy 9 (1995) 619.
[8] P. Rowntree, L. Parenteau, L. Sanche, J. Chem. Phys. 94 (1991) 8570.
[9] M. Tronc, R. Azria, Y. Le Coat, E. Illenberger, J. Phys. Chem. 100 (1996) 14745.
[10] G.A. Kimmel, T.M. Orlando, Phys. Rev. Lett. 77 (1996) 3983.
[11] W.C. Simpson, L. Parenteau, R.S. Smith, L. Sanche, T.M. Orlando, Surf. Sci. 390 (1997) 86.
[12] W.C. Simpson, M.T. Sieger, T.M. Orlando, L. Parenteau, K. Nagesha, L. Sanche, J. Chem. Phys. 107 (1997) 8668.
[13] W.C. Simpson, T.M. Orlando, L. Parenteau, K. Nagesha, L. Sanche, J. Chem. Phys. 108 (1998) 5027.
[14] G.A. Kimmel, T.M. Orlando, C. Vézina, L. Sanche, J. Chem. Phys. 101 (1994) 3282.
[15] L. Sanche, L. Parenteau, J. Chem. Phys. 93 (1990) 7476.
[16] G.B. Fisher, J.L. Gland, Surf. Sci. 94 (1980) 446.
[17] R.S. Smith, C. Huang, E.K.L. Wong, B.D. Kay, Surf. Sci. 367 (1996) L13.
[18] P. Löfgren et al., Surf. Sci. 367 (1996) L19.
[19] K.-D. Rinnen et al., J. Chem. Phys. 95 (1991) 214.
[20] I.N. Levine, Quantum Chemistry, Prentice Hall, Englewood Cliffs, 1991.
[21] W.A. Goddard III, W.J. Hunt, Chem. Phys. Lett. 24 (1974) 464.
[22] D.S. Belic, M. Landau, R.I. Hall, J Phys. B: At. Mol. Phys. 14 (1981) 175.
[23] M. Jungen, J. Vogt, V. Staemmler, Chem. Phys. 37 (1979) 49.
[24] M.G. Curtis, I.C. Walker, J. Chem. Faraday Trans. 88 (19) (1992) 2805.

[25] M.T. Sieger, T.M. Orlando, Surf. Sci. 390 (1997) 92.
[26] M.T. Sieger, W.C. Simpson, T.M. Orlando, Phys. Rev. B 56 (1997) 4925.
[27] V. Buch (private communication).
[28] M.J. Idema et al., J. Phys. Chem. B 102 (1998) 9203.
[29] H. Dosch, A. Lied, J.H. Bilgram, Surf. Sci. 327 (1995) 145.
[30] P.J. Wooldridge, J.P. Devlin, J. Chem. Phys. 99 (1988) 3086.
[31] D.E. Brown et al., J. Phys. Chem. 100 (1996) 4988.
[32] A. Balková, R.J. Bartlett, J. Chem. Phys. 99 (1993) 7907.
[33] S. Klen, E. Kochanski, A. Trich, A.J. Sadlej, Theor. Chim. Acta 94 (1996) 75.
[34] R.A. Rosenberg, P.R. LaRoe, V. Rehn, J. Stöhr, R. Jaeger, C.C. Parks, Phys. Rev. B 28 (1983) 3026.
[35] G.A. Kimmel, T.M. Orlando, (unpublished).
[36] D. Betowski, J.D. Payzant, G.I. Mackay, D.K. Bohme, Chem. Phys. Lett. 31 (1975) 321.
[37] C.E. Klots, R.N. Compton, J. Chem. Phys. 69 (1978) 1644.
[38] M. Knapp, O. Echt, D. Kreisle, E. Recknagel, J. Phys. Chem. 91 (1987) 2601.